Differentiating Clayey Soil Layers from Electrical Resistivity Imaging (ERI) and Induced Polarization (IP)

Dr. Hussein H. Karim
Building and Construction Engineering Department, University of Technology/Baghdad
Email:husn_irq@yahoo.com
Dr. Dr. Mahmoud R. AL- Qaissy
Building and Construction Engineering Department, University of Technology/ Baghdad
Nadia A. Aziz

Received on: 27/1/2013 & Accepted on: 11/6/2013

ABSTRACT

Electrical Resistivity Imaging (ERI) method is one of the most promising techniques which is well suited for the applications in the fields of geohydrology, environmental science and engineering. The present work is aimed to show the efficiency of 2D Electrical Resistivity Imaging (ERI) and Induced Polarization (IP) in probing the subsurface soil for site investigation and differentiating the clayey soil layers as it is a common practice to measure the IP sounding along with resistivity for correct interpretation of field data. The study has demonstrated the practical application of 2D ERI and IP tomography along 7 lines using Wenner- Schlumberger array. The data analysis comprises of 2D inversions using the RES2DINV software, thus 2D electrical resistivity and IP imaging sections have been obtained. The depth of investigation was 4 m, and resistivity values range from <1 to 292 ohm.m. Two electrical layers were recognized: the upper layer with high resistivity (7-71 ohm.m) represents the loamy soil extends to a depth around 1.3 m; and the second layer with low resistivity (<1-9 ohm.m) represents the clayey layer. Some anomalous low and high electric zones are appeared reflecting the inhomogeneity in deposits. The IP values are ranging from -2 to 17 mV/V showing good confirmation with resistivity data, where high chargeability are associated with low resistivity. The study reveals that combining IP with resistivity surveys is recommended since IP is, sometimes, very effective in relieving ambiguity in interpretation.

Keywords: 2D Electrical resistivity imaging (2D-ERI); IP Imaging; Chargeability; Clayey Soil; Site Investigation.

https://doi.org/10.30684/etj.31.17A.1
2412-0758/University of Technology-Iraq, Baghdad, Iraq

تمييز طبقات التربة الطينية من المقاومة النوعية الكهربائية (ERI) التصويرية (IP)والاستقطاب المستحث

الخلاصة

طريقة المقاومة النوعية الكهربائية التصويرية (ERI) هي واحدة من التقنيات الواعدة المناسبة تماما للتطبيقات في مجالات العلوم والهندسة البيئية والهيدروجيولوجية. يهدف هذا العمل لإظهار كفاءة المقاومة النوعية الكهربائية التصويرية (ERI) والاستقطاب المستحث (IP) في جس التربة تحت السطحية للتحري الموقعي وتمييز طبقات التربة الطينية والذي يعد ممارسة شائعة لقياس الاستقطاب المستحث التصويري IP جنبا إلى جنب مع المقاومة النوعية لغرض التفسير الصحيح للبيانات الحقلية . أظهرت الدراسة التطبيق العملي لل (2D-ERI) والتصوير المقطعي ل(IP) على طول 7خطوط باستخدام ترتيب فنر-شلمبرجير. يتألف تحليل البيانات من انعكاسات 2D باستخدام برنامج RES2DINV، وبالتالي الحصول على مقاطع المقاومة النوعية الكهربائية والاستقطاب المستحث التصويرية ثنائية الأبعاد. بلغ عمق التحري٤ متر،وتراوحت قيم المقاومة النوعية (<1to 292ohm.m).

تم التعرف على طبقتين كهربائيتين: الطبقة العليا ذات مقاومة نوعية عالية (7-71ohm.m) تمثل التربة الطمية وتمتد إلى عمق نحو١,٣ مترا، والطبقة الثانية ذات مقاومة نوعية منخفضة (1-9< ohm.m) وتمثل الطبقة الطينية. ظهرت بعض المناطق الكهربائية الشاذة المنخفضة والعالية والتي تعكس عدم التجانس في الرسوبيات. وتراوحت قيم IP ما بين (-2 to 15 mV/V) وبتوافق جيد مع بيانات المقاومة النوعية، حيث ترتبط قابلية الشحن (chargeability) العالية مع المقاومة النوعية المنخفضة .وتكشف الدراسة الى توصية مفادها ان الجمع ما بين IP والمقاومة النوعية هو، في بعض الأحيان، فعال جدا في تخفيف الغموض في التفسير.

INTRODUCTION

Resistivity values of earth materials cover a wide range. The variety of resistivity has been the essential reason why the technique can be used for different applications [1].

Electrical Resistivity Imaging (ERI) is one of the most promising techniques which is well suited to applications in the fields of geohydrology, environmental science and engineering [2, 3]. There have been many applications of electrical resistivity methods for detecting sinkholes and cavities, walls and other man-made structures that were not previously possible with conventional 1D resistivity surveys, for example, see Burger (1992) [4]; Maillol et al. (1999) [5], and Van Schoor (2002) [6].

ERI is a geophysical technique that calculates the subsurface distribution of soil electrical resistivity. Electrical resistivity ($\rho, \Omega m$), a measure of the ability of a body to limit the transfer of electrical current, is defined in cylindrical geometry as:

$$\rho = R\frac{S}{L} \qquad \ldots (1)$$

Where R is electrical resistance (Ω), *S* is cross-sectional area of the cylinder (m^2) and *L* is the length of the cylinder (m). Soil resistivity surveys are conducted by applying electric currents to the soil through conductors (electrodes) and measuring the

resulting differences in electric potential (voltage) at selected positions in the soil [7]. The distribution in space of voltage differences is a function of the different resistivity of soil volumes [8]. There are different electrode configurations, called electrode arrays where the electrical current (*I*) is injected by two electrodes conventionally named '*A*' and '*B*' and the potential difference (ΔV) is measured by two other electrodes '*M*' and '*N*'. The measured electrical resistivity (received voltage over the transmitted current, multiplied by a geometric factor k) of the prospected medium is called apparent resistivity (ρ_a) because each value corresponds to an integrated volume, and is calculated by:

$$\rho_a = \frac{\Delta V}{I} \frac{2\pi}{\frac{1}{AM} - \frac{1}{BM} + \frac{1}{BN} - \frac{1}{AN}} \quad \ldots (2)$$

Where *AM* (*BM*, *BN*, *AN*, respectively) represents the distance between electrodes *A* and *M* and (*B* and *M*, *B* and *N*, *A* and *N*, respectively) (Fig. 1a) [9, 10]. Denoting $2\pi / \left(\frac{1}{AM} - \frac{1}{BM} + \frac{1}{BN} - \frac{1}{AN}\right)$ by k the above equation becomes:

$$\rho_a = kR \quad \ldots (3)$$

k is the geometric factor and only a function of the geometry of the electrode arrangement. Resistivity can be found from measuring values of *V*, *I* and k. By increasing the distance between all four electrodes, the depth of investigation increases and deeper zones in the soil profile can be characterised [9].

A 2D subsurface resistivity model provides more accurate subsurface imaging as in Figure (1 b). The resistivity varies in both the vertical direction and the horizontal direction along the survey line. In the 2D case, it is assumed that subsurface resistivity does not change in the direction perpendicular to the survey line. Such surveys are usually carried out using a large number of electrodes connected to a multi–core cable. A laptop computer together with an electronic switching unit is used to automatically select the four electrodes for each measurement. In recent years, field techniques and the equipment to carry out efficient 2D resistivity surveys have become fairly well developed.

For geophysical applications, in certain conventional resistivity surveys we can note that the potential difference, measured between the potential electrodes, do not drop instantaneously to zero when the current is turned off. Instead, the potential difference drops sharply at first, then gradually decays to zero after a given interval of time. This means that certain bodies in the ground can become electrically polarized, forming a battery when energized with an electric current. Upon turning off the polarizing current, the ground gradually discharges and returns to equilibrium. This phenomenon is the foundation of a geophysical survey technique called Induced

Polarization (IP) [11]. The IP method is widely used in exploration for ore bodies, principally of disseminated sulfides. The IP method is also used in groundwater exploration to discriminate between the salt water layers and clay, and for the study of pollutants in the ground [11].

The present work is aimed to show the efficiency of 2D Electrical Resistivity Imaging (ERI) and Induced Polarization (IP) in probing the subsurface soil and differentiating the clayey soil layers as it is a common practice to measure the IP sounding along with resistivity for correct interpretation of field data.

D ERI AND IP MEASUREMENTS

Electrical resistivity and induced polarization tomography techniques are increasingly used for a wide range of environmental and engineering geophysics problems.

ERI is a proven imaging technique where the theory and application are well documented in geophysical research literature (such as Griffiths and Barker, 1993 [12]; Daily and Owen, 1991 [13]; Daily and Ramirez, 1992 and 1995[14, 15]).

Survey design and layout strategies that produce optimum information using different ERI configurations and set up in different geological settings have been the topic of several studies (e.g., Alumbaugh and Newman, 1999 [16]; Stummer et al., 2004 [17]). The electrode configuration used in our surveys was the Wenner-Schlumberger array Figure (1a): four electrodes were arranged in line, with A and B electrodes at the external positions and M and N electrodes in between. Such surveys are usually carried out using a large number of electrodes connected to a multi–core cable. A laptop computer together with an electronic switching unit is used to automatically select the four electrodes for each measurement. In recent years, field techniques and the equipment to carry out efficient 2D resistivity surveys have become fairly well developed. Generally a constant spacing between adjacent electrodes is used. The multi–core cable is attached to an electronic switching unit which is connected to a laptop computer or has a built–in computer. The sequence of measurements to take, the type of electrode array to use, and other survey parameters is programmed into the computer. After reading the control file, the system automatically selects the appropriate sequence of electrodes to complete the measurements. Most of the fieldwork is involved in laying out the cable and electrodes. After that, the measurements are taken automatically and stored in the computer. A significant amount of the survey time is spent waiting for the resistivity meter to complete the set of measurements. The roll–along survey technique is now widely used in resistivity surveys to extend horizontally data coverage, particularly for a resistivity system with a limited number of cables and electrodes. After completing the initial sequence of measurements, the cable is moved past one end of the line by several unit electrode spacing's. All the measurements which involve the electrodes on the part of the cable which does not overlap the original end of the survey line are then repeated of measurements used to build up a pseudosection [18].

For the characterisation of the soil cultivated layer, a 2D electrical profile was constructed. A 2D subsurface resistivity model provides more accurate subsurface

imaging. The resistivity varies in both the vertical direction and the horizontal direction along the survey line. In the 2D case, it is assumed that subsurface resistivity does not change in the direction perpendicular to the survey line.

To be correctly interpreted, the measured integrated values must be converted so they can then be correlated to the resistivity parameter and to other soil characteristics. This conversion can be made by inversion software and the results are then called 'inverted resistivities'. The RES2DINVsoftware was used in this case to calculate a distribution map of inverted resistivity. At each point of the map, the inverted resistivity value corresponds to the value of resistivity at that location, without any integration. Final 2D plots were obtained after linear interpolation. Several parameters related to soil characteristics (i.e. porosity, water content, clay content, salinity) or climatic conditions (temperature) can influence electrical resistivity values.

Numerical modeling or some measure of the Jacobian matrix of partial derivatives is usually used to quantitatively evaluate sensitivity of datasets and to assess the resolution of the resistivity images. The resolution information is not only useful in designing field experiments, but also it is helpful when interpreting resistivity models derived from inversion processes. It can be used to identify artifacts in the model and the level to which the details can be interpreted within the model [10].

Recent advances in IP instrumentation and modeling algorithms, combined with a better understanding of the physical significance of the IP response, encourages field-scale engineering applications of the method. Within the last 10 years, a revolution in the application of the resistivity method occurred with development of multi-electrode, automated data acquisition systems and 2D (recently 3D) inversion algorithms for resistivity image reconstruction. Engineering and environmental applications of the resistivity method escalated as a result of these technological advances, which facilitate visualization of the subsurface resistivity distribution. In recent years, this technology has been extended to upgrade the IP method. Instrumentation and software now exist, making it possible to obtain 2D or 3D images of the polarizability of the subsurface [19].

By calculating soil resistivity, it is possible detect water, clay layers, voids, but it is also possible to reconstruct sections of the ground that can be used to select and calibrate the parameters for GPR surveys [10].

GEOELETRICAL INVESTIGATIONS AND SURVEY DESIGN

The field work was carried out in the football field site located in the University of Technology in Baghdad (Figure (2)). The electrical imaging and IP surveys were achieved between February 27, 2012 to May 3, 2012. The 2D resistivity imaging was conducted along survey W-E lines (1, 2, 3, 4, 5, 6 and 7) with 20 m in length for each line, with an inter-electrode spacing of 0.5 m using the Wenner-Schlumberger Array Figure (3). The line spacing was 7 m for all lines except that between lines 6 and 7, where it was 5 m.

Electrical Resistivity Imaging Survey

ERI survey data were acquired using ABEM SAS-4000 Lund Imaging System with 64 electrodes connected to a multi-core cable [12]. With this equipment,

consecutive readings were taken automatically and the results averaged continuously. SAS results are more reliable than those obtained using manually operated single-shot systems (ABEM, 2008)[20], because the latest equipment is an automated machine connected with a laptop with an electronic switching unit that automatically selects the relevant four electrodes for each measurement [1,21]. Wenner-Schlumberger configuration was chosen for its high resolution and depth of penetration [21]. The data was processed and inverted using RES2DINVsoftware. The program generates the inverted resistivity-depth image for each profile line.

IP Survey Method

It is a common practice to measure the IP sounding along with resistivity for correct interpretation of field data. Induced Polarization data were also acquired using the same SAS-4000 ABEM Terrameter with the same electrode configuration in the multi-electrode resistivity meter system. Measuring IP with ERI enables us to interpret the data in 2D as well as using the RES2DINVsoftware. This robust attempt is one of the more recent developments in the instrumentation of electrical imaging surveys [21, 22].

RESULTS AND INTERPRETATION

2D Inverted Resistivity and IP Section Results

The raw field data or measured apparent resistivity data were processed using RES2DINV. This computer program uses a least squares inversion to convert the measured apparent resistivity values to true resistivity values and plots them in cross section. The program creates a resistivity cross-section, calculates the apparent resistivities for that cross-section, and compares the calculated apparent resistivities to the measured apparent resistivities. The iteration continues until a combined smoothness constrained objective function is minimized.

The results for 2D and their corresponding IP tomographs Figures (4 to 10) demonstrate that the maximum depth of investigation ranged between 3.7 to 4.8 m. The resistivity values range between < 1 to 292 ohm.m with RMS 1.3-12.6% after 2-7 iterations. While the IP values range between -2 to 17 mV/V with RMS 0.6-1.7% after 5-10 iterations. The detailed 2D inverted resistivity and IP sections results and explanation of each line as follows:

LINE 1

The 2D inversion resistivity pseudosection of Line 1 Figure (4a) shows that the resistivity values vary from 0.7 to 55.1 ohm.m with 12.6 % RMS after 2 iterations. In this profile, the uppermost is with relatively high resistivity value ranging from 8.5 to 55.1 ohm.m, especially at the right side. In the deeper layer, the resistivity value ranges from 0.69 to 2.4 ohm.m appeared in blue color, and it was interpreted as clay. At the center of the profile, a distinguishable zone with a high resistivity value was noticed at depth 0.09 m down to 0.5 m with a maximum value around 55.1 ohm.m. This anomaly could be explained as possible dry sand.

The IP values for the same profile vary between -2 to 17 mV/V with 1.7% RMS after 6 iterations as shown in Figure (4b). The IP values distribution shows a homegenuos pattern except for an area located at a depth of 1.25 m down to 2.48 m

with a maximum value of around 17 mV/V with high chargeability in the IP profile (compared with low resistivity values in the resistivity profile), this area was interpreted as a soft clay.

LINE 2

The resistivity values of the 2D inversion resistivity pseudosection of LINE 2 vary between 0.6 and 292 ohm.m with RMS of 10.3 % after 3 iterations Figure (5a). The subsurface resistivity image along Line 2 appears similar to that obtained from Line 1 with the same appeared layers. The profile shows one distinguishable small zone, which is also appeared in Line 1, with a high resistivity value (with a maximum value around 292 ohm.m) situated at the center of the profile at a depth of 0.09 m down to 0.5 m. This anomaly is interpreted as possible dry sand.

The IP values vary between -1.5 and 3.67 mV/V with RMS of 1.5 % after 10 iterations see Figure (5b). The IP profile presents mainly two distinguishable zones with high IP effect. The first one occurs between the horizontal distance -1 and 3 m along the spread line and a depth ranged from 0.7 m down to 3.8 m with IP value around 3.7 mV/V. While, the second zone located between -3 m and -6 m along the spread line and at a depth 0.67 m down to 2.4 m. This is consistent with the previous interpretation. This zone may be a clayey zone which causes a high IP-effect.

LINE 3

The subsurface resistivity image along Line 3 see Figure (6a) appears similar to that resulted from Line 2, except some details. The resistivity values from the inversion of the field data vary from 0.29 to 89.4 ohm.m with RMS of 9.9% after 3 iterations. The local high resistivity zones appeared in both Lines 1 and 2 are also shown in this profile. These anomalous zones are located at the center of the profile with a maximum value around 89.4 ohm.m which might represent dry sands.

The IP values vary between -0.7 and 2.2 mV/V with RMS of 1.4 % after 10 iterations as shown in Figure (6b). It is noticed in this figure that the proposed clay area appeared previously in the resistivity section in blue color see Figure (6a) is also shown in the IP section in yellow color with slightly higher chargeability than its surroundings, supporting its proposition as a clay area. Besides, other two main zones (brown color) appeared in both the resistivity and IP profiles at 1.5 m in depth with minimum resistivity value (0.29 ohm.m) in contrast to its accompanied high chargeability (2.26 mV/V), are interpreted as possible soft clay.

LINE 4

The resistivity values for this line vary between 0.18 and 99.2 ohm.m with RMS of 8.7 % after 3 iterations see Figure (7a). It is noticed, as found in lines 1 to 4, that there is a similarity in the resistivity section with an inhomogenous pattern showing the highest resistivity values in the superficial layer (loamy soil) followed by a lowest resistivity values (clayey layer).

The IP values between 1.4 and 10.2 mV/V with RMS of 1.1 % after 10 iterations see Figure(7b).The proposed clay area that appeared previously in the resistivity section

(blue color) as shown in Figure(7a) is also shown in the IP profile (light green color) with slightly higher chargeability than its surroundings, supporting its proposition as a clay area. While, the other two main brown zones appeared in both the resistivity and IP sections, at a depth of 1.25 m with minimum resistivity value (0.18 ohm.m) in contrast to its associated high chargeability (4.25 mV/V), are interpreted as soft clay.

LINE 5

The resistivity values vary between 1.42 and 71.9 ohm.m see Figure (8a) with RMS of 2.2 % after 7 iterations. This section reveals two different layers; the first layer shows high resistivity value ranging from 41 to 71.9 ohm.m with depth around 0.6 m, and this layer may represent the loamy soil. While, the second one exhibits lower resistivity values ranging from 1.42 to 7.65 ohm.m which could be interpreted as a clayey layer.

The IP values for this line vary between 0.6 and 2.7 mV/V with RMS of 0.9 % after 7 iterations see Figure (8b). Three anomalous zones appeared in both resistivity and IP profiles, all with minimum resistivity value of 1.42 ohm.m in contrast to its associated high chargeability (0.6 mV/V), could refer to the soft clay.

LINE 6

In this section, the resistivity values ranged from 1.7 to 67.5 ohm.m with RMS of 1.48 % after 7 iterations as shown in Figure (9a). The inversion resistivity image shows two different layers; the first layer is of high resistivity ranges from 13.6 to 67.5 ohm.m at depth around 0.6 m from the ground surface which may refer to the loamy soil. The second layer exhibits resistivity values ranging from 1.61 to 7.9 ohm.m and could be represented as clayey layer. This section showed two distinguishable zones. The first one with a high resistivity value occurs at the right side of the profile at depth 0.09 m down to 0.66 m with a maximum value around 67.5 ohm.m. These anomalies may represent possible cavity to dry sand. While, the second one occurs at the left side of the profile at depth 0.66 m down to 1.86 m with resistivity value of 2.75 ohm.m . This zone may be assigned to the soft clay.

The IP values is within -0.04 mV/V with RMS of 0.6% after 5 iterations Figure (9b). This spread is quite homogenous, and this may be explained by a high water content of this zone due to irrigation of this field one day prior to investigation.

LINE 7

The resistivity values range from 1 to 29 ohm.m with RMS of 1.31% after 7 iterations as depicted in Figure (10a). The inversion resistivity section showed two different layers; the first layer is of high resistivity ranging from 13 to 29 ohm.m at depth of about 0.6 m which may refer to the loamy soil with higher values at both ends possibly referring to the presence of small cavities or sand. While the second one characterizes by its lower resistivity values ranging from 1 to 9 ohm.m and may be represented as a clayey layer. This section exhibits one main distinguishable zone occurs at the left side of the profile at depth 0.6 m down to 2.0 m with resistivity value around 3 ohm.m. This zone may be explained as soft clay which is also appeared in Lines 5 and 6.

The IP values vary between -1 and 15 mV/V with RMS of 0.78 % after 7 iterations Figure (10b). Two distinguishable zones appeared in both the resistivity and IP profiles, both with minimum resistivity value (1 ohm.m) in contrast to its associated high chargeability (7 mV/V) which are explained as soft clay.

CONCLUSIONS

1. The study has demonstrated the practical application of 2D ERI and IP tomography, along 7 lines using Wenner-Schlumberger array, in characterizing the subsurface soil for engineering site investigation.
2. Interpretation of 2D ERI images has revealed that the subsurface soil at the study site is mainly clayey soil with resistivity values range from <1 to 292 ohm.m with an average depth of investigation is 4 m. Two electrical layers were recognized as follows: the upper with high resistivity (7-71 ohm.m) represents the loamy soil to depth around 0.6 m, while the lower one of low resistivity (<1-9 ohm.m) represents a clayey layer.
3. Some anomalous low and high electric zones appeared reflecting the inhomogeneity in deposits. Of these; high resistivity zone (68 ohm.m at depth <1- 1 m) which may refer to the possible dry sand. The others are with low resistivity (2.8-7.7 ohm.m at depth <1- 3 m) which may represent the soft clay.
4. The IP values are ranging from -2 to 17 mV/V with high chargeability (low resistivity) for soft clay. While low chargeability corresponds to high resistivity in the resistivity sections for the same site. The soft clay zones appeared with relatively high chargeability (around 2.5-4.3 mV/V) at depths from the near surface to about 2.5 m in depth. Some spreads appeared with very low chargeability (-0.04 mV/V) referring to high water content due to irrigation.
5. By comparing resistivity and IP studies, it was noted that resistivity measurements are better in distinguishing different materials, but IP-measurements are a good complement to resolve ambiguities in the interpretation, it is an indicator of clay content which be acquired simultaneously with resistivity without extra cost.
6. Combining IP with resistivity surveys is recommended since IP is, sometimes, very effective in relieving ambiguity in interpretation.

REFERENCES

[1]. Loke, M.H., "Electrical Imaging Surveys for Environmental and Engineering Studies: A Practical Guide to 2D and 3D Surveys", 2000.

[2]. Spies, B., Ellis, R., "Cross-borehole resistivity tomography of a pilot sale, in-situ vitrification test", Geophysics, V. 60, pp.886– 898, 1995.

[3]. Barker, R., Moore, J., "The application of time-lapse electrical tomography in groundwater studies", Lead. Edge, V. 17, No.10, pp.1454–1458, 1998.

[4]. Burger, H.R., "Exploration Geophysics of the Shallow Subsurface", Prentice-Hall, Englewood Cliffs, NJ, 489 P., 1992.

[5]. Maillol, J.M., Seguin, M.-K., Gupta, O.P., Akhauri, H.M., Sen, N., " Electrical resistivity tomography survey for delineating uncharted mine galleries in West Bengal, India", Geophys. Prospect., Eur. Assoc. Geosci. Eng., V. 47, pp.103– 116, 1999.

[6]. Van Schoor, M., Detection of sinkholes using 2D electrical resistivity imaging Journal of Applied Geophysics, V.50, pp. 393– 399, 2002, . www.ivsl.org.

[7]. Amato, M., Basso, B., Celano, G., Bitella, G., Morelli, G. and Rossi, R., "In situ detection of tree root distribution and biomass by multielectrode resistivity imaging", Tree Physiology V. 28, pp. 1441-1448, 2008, www.ivsl.org.

[8]. Kearey P, Brooks M, Hill I, "An introduction to geophysical exploration", Blackwell Science, Oxford, 2002.

[9]. Besson A., Cousin I., Samouëlian A., Boizard H., Richard G.,"Structural heterogeneity of the soil tilled layer as characterized by 2D electrical resistivity surveying",Soil&Tillage Research V.79, pp.239–249, 2004, doi: 10.1016/j.still.2004.07.012.

[10]. Zenone, T., Morelli,G., Teobaldelli, M., Fischanger,F., Matteucci,M., Sordini, M., Armani,A., Ferrè,C., Chiti, T. and Seufert, G., "Preliminary use of ground-penetrating radar and electrical resistivity tomography to study tree roots in pine forests and poplar plantations", Functional Plant Biology, V. 35, pp.1047–1058, 2008, www.ivsl.org.

[11]. Marescot,L.,"Engineering and Environmental Geophysics", Ingenieur- und Umweltgeophysik, lecture given at the ETH Zurich, 2005.

[12]. Griffiths, D.H., Barker, R.D.," Two-dimensional resistivity imaging and modeling in areas of complex geology", J. Appl. Geophys., V. 29, pp.211– 226, 1993.

[13]. Daily, W., Owen, E., " Crosshole resistivity tomography", Geophysics, V. 56, pp.1228– 1235, 1991.

[14]. Daily, W., Ramirez, A., " Electrical resistivity tomography of vadose water movement", Water Resour. Res. , V.28, pp.1429– 1442, 1992.

[15]. Daily, W., Ramirez, A., "Environmental process tomography in the United States", Chem. Eng. J. , V.56, pp.159– 165, 1995.

[16]. Alumbaugh, D.L. and Newman, G.A., "Image appraisal for 2-D and 3-D electromagnetic inversion",In: Proceedings of the Society of Exploration Geophysicists Annual Meeting, New Orleans,1998, New Orleans, Louisiana, The Society of Exploration Geophysicists, pp. 2–10, 1999.

[17]. Stummer,P., Maurer,H. and Green, A.G., "Experimental design: Electrical resistivity data sets that provide optimum subsurface information", Geophysics, V. 69, No. 1, pp.120–139, 2004.

[18]. Loke, M. H. and Barker, R. D., "Rapid least–squares inversion of apparent resistivity pseudosections by a quasi–Newton method", Geophysical Prospecting, V. 44, pp. 131–152, 1996.

[19]. Slater, L.D. and Lesmes, D., "The induced polarization method", In: proceedings of the first international conference on the application of geophysical

methodologies & NDT to transportation facilities and infrastructure, December 2000, St. Louis, Missouri, 2000.

[20]. ABEM, "Instruction Manual for Terrameter SAS 1000/4000", ABEM Instrument AB, Sundbyberg, Sweden. 135P., 2008.

[21]. Loke M.H.,"Tutorial: 2-D and 3-D Electrical Imaging Surveys", 2004 Revised Edition. 136P. 2004, www.geometrics.com.

[22]. Murali, S. and Patangay, N. S., "Principles of Application of Groundwater Geophysics", Association of Geophysicists, Hyderabad, India, 3rd Ed. 371P., 2006.

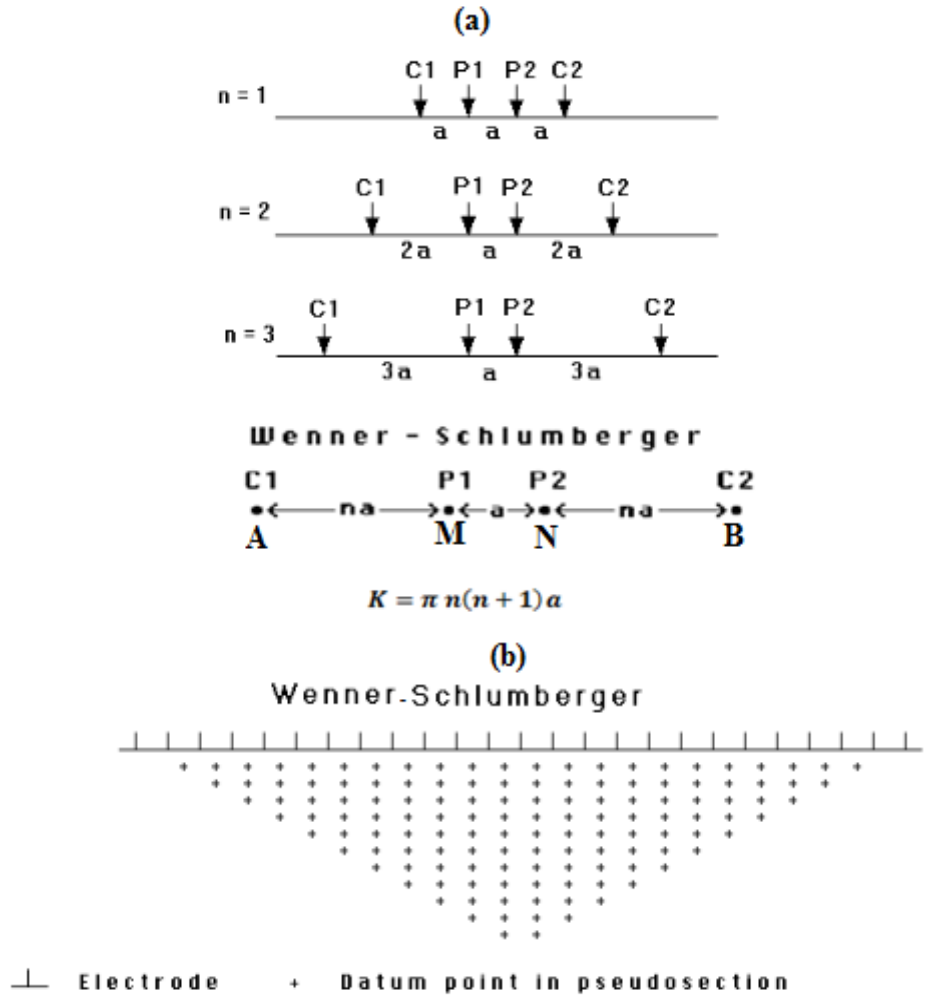

Figure (1) A comparison of the (a) electrode arrangement and (b) 2-D pseudo section data pattern for the Wenner-Schlumberger arrays (Modified after Loke, 2000 [1]).

Figure (2) Football field site of the University of Technology.

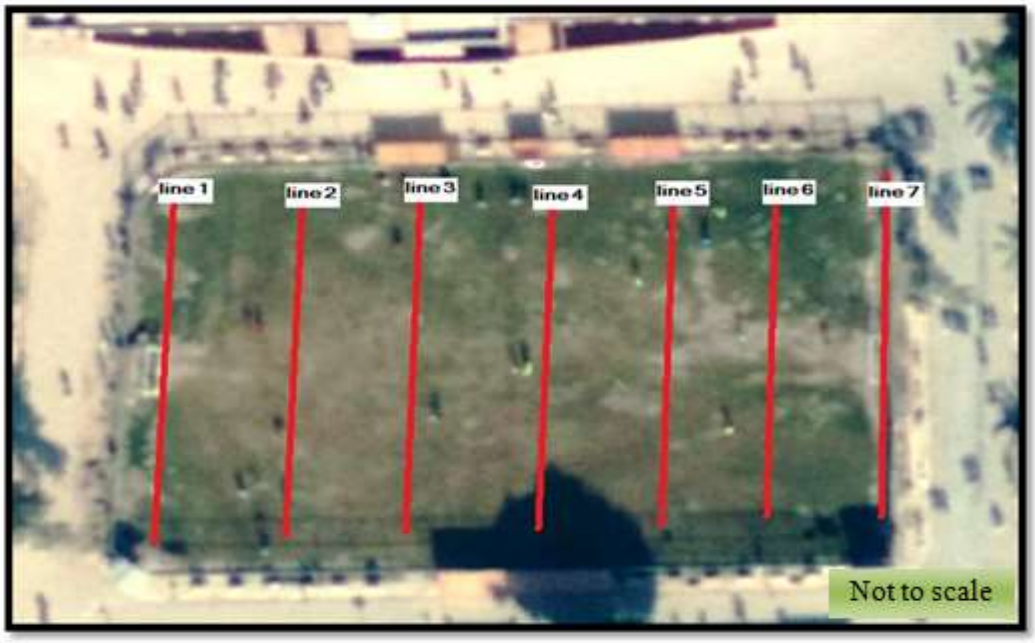

Figure (3) Acquisition geometry for resistivity and IP survey in the site.

(a)

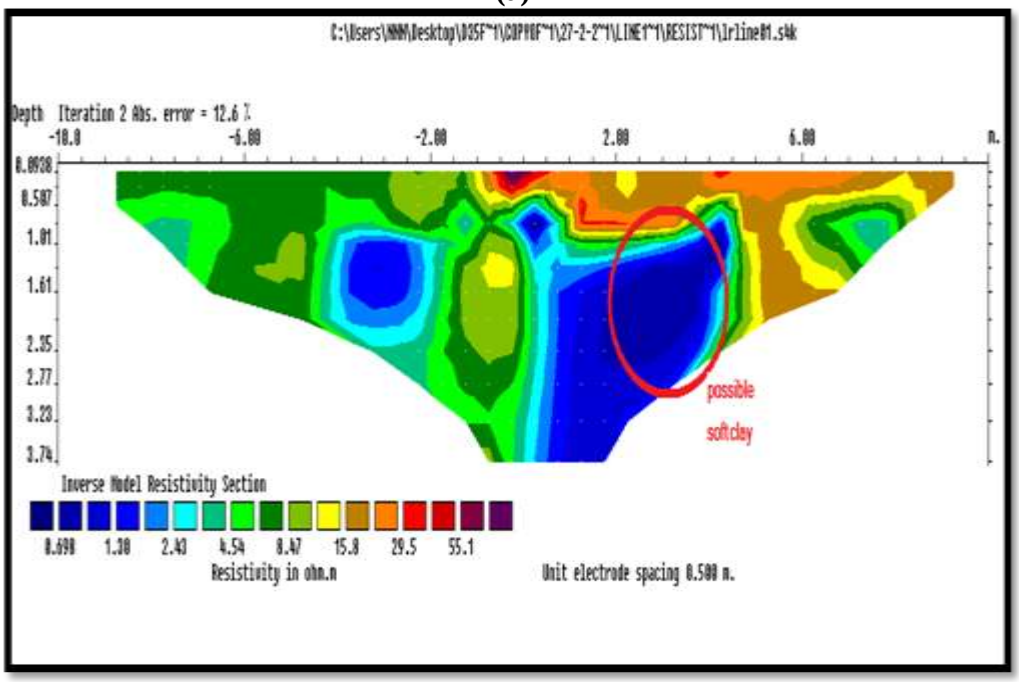

(b)

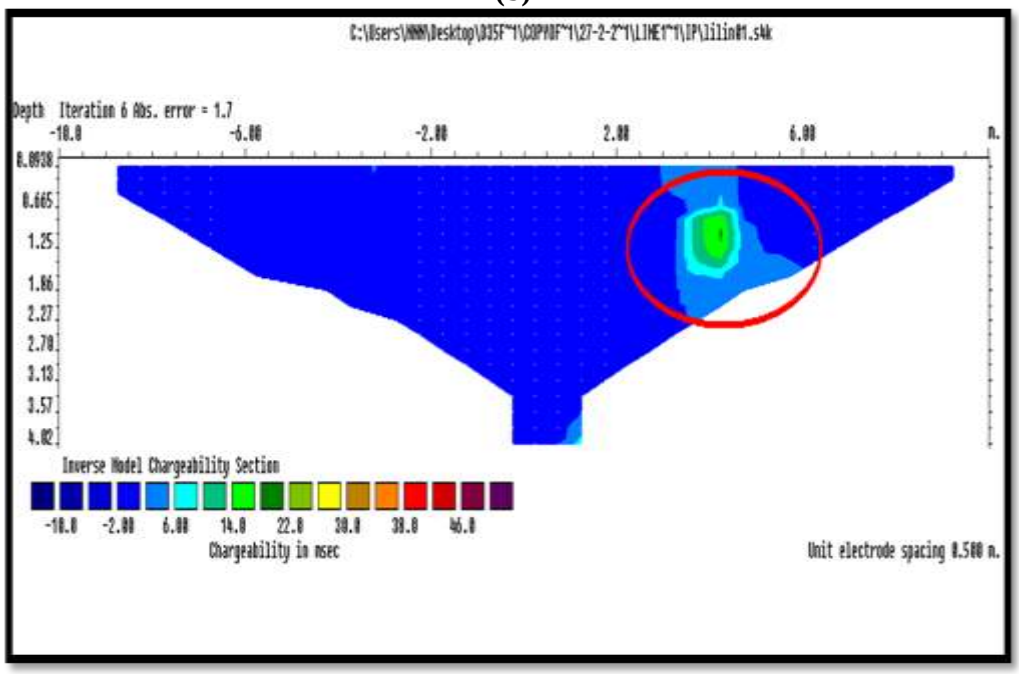

Figure (4) Inverted sections of LINE 1: (a) resistivity; (b) chargeability.

(a)

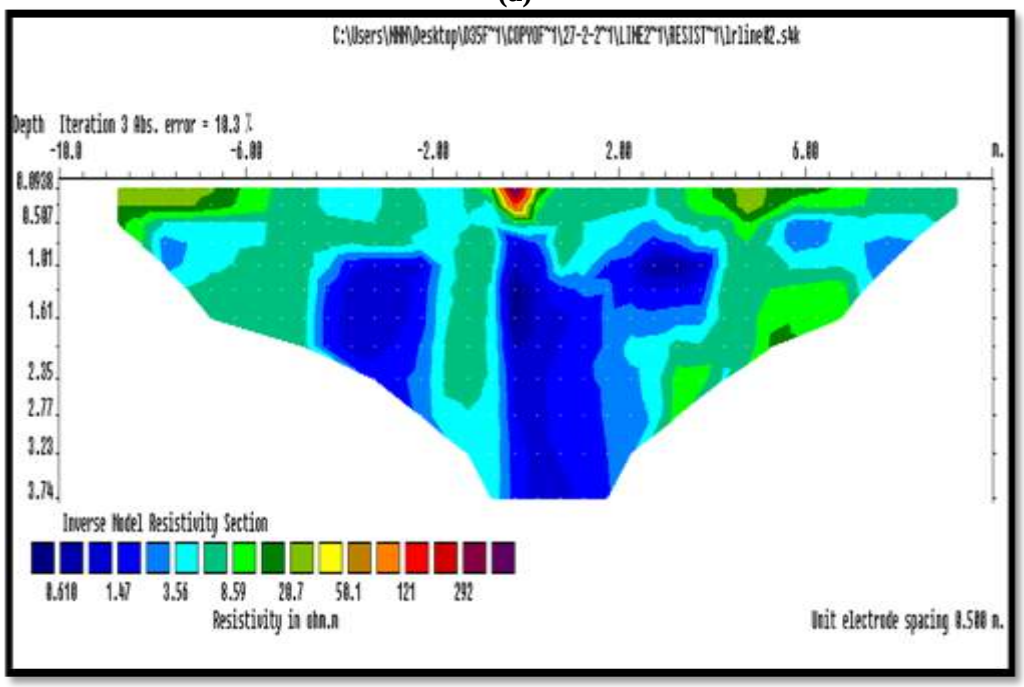

(b)

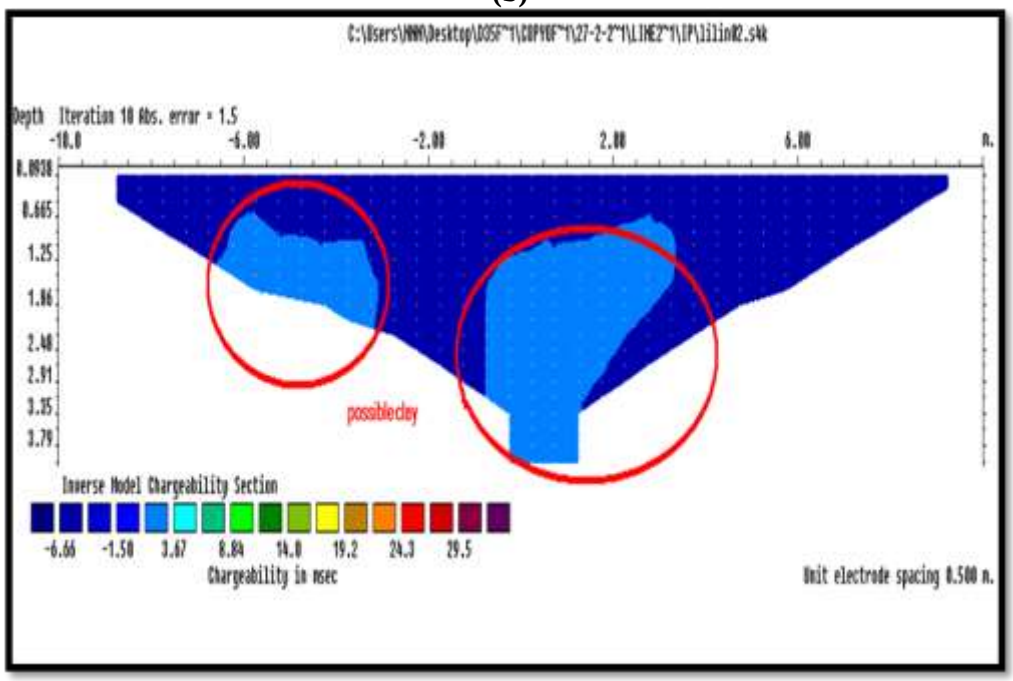

Figure (5) Inverted sections of LINE 2: (a) resistivity; (b) chargeability.

(a)

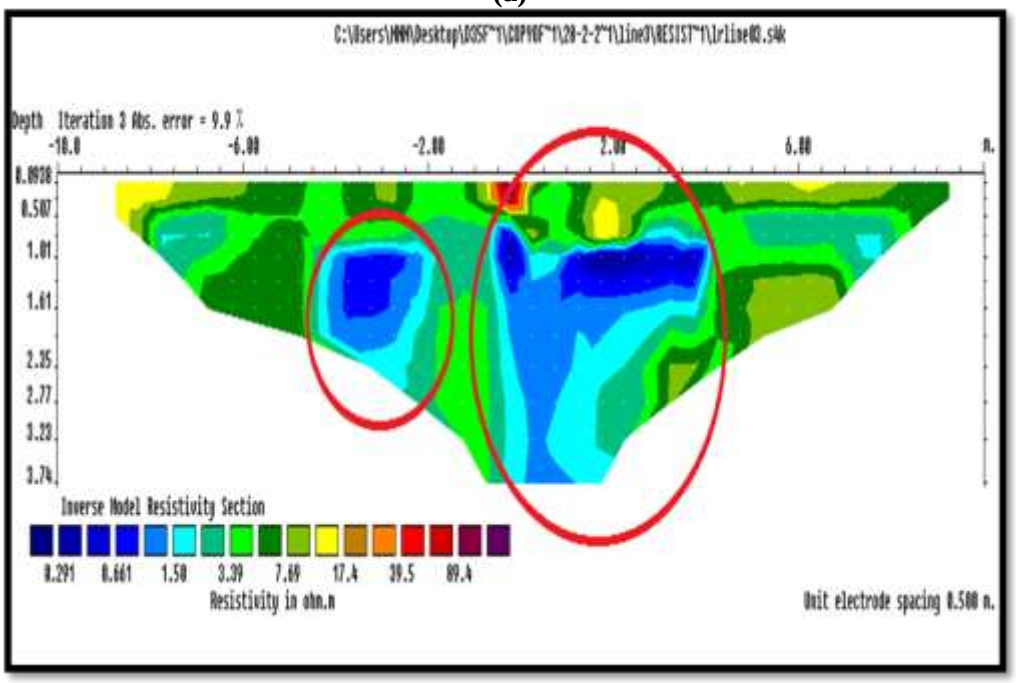

(b)

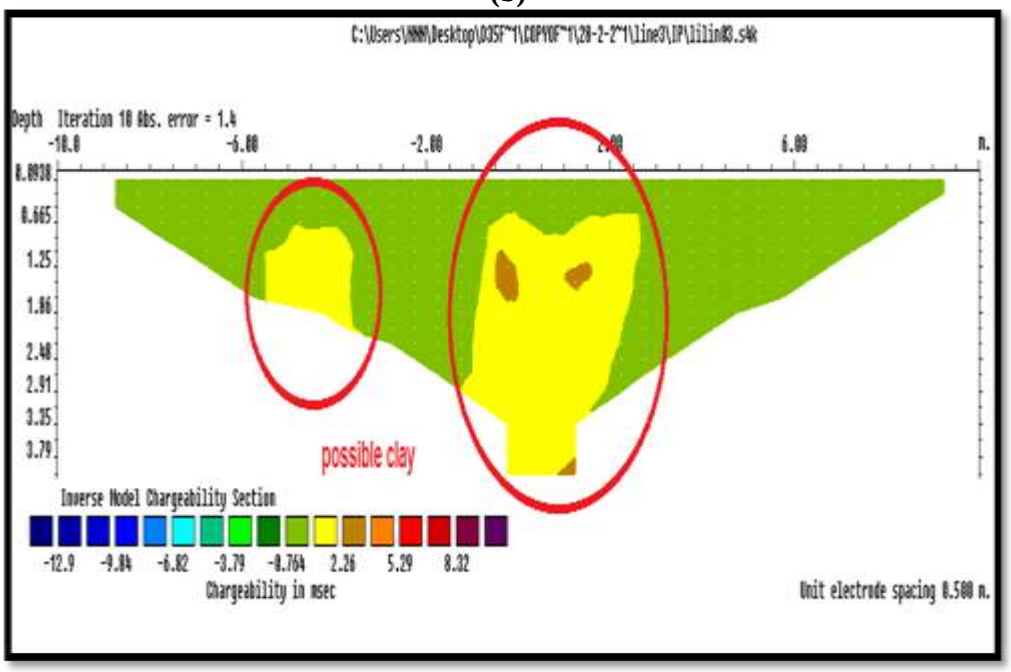

Figure (6) Inverted sections of LINE 3: (a) resistivity; (b) chargeability.

(a)

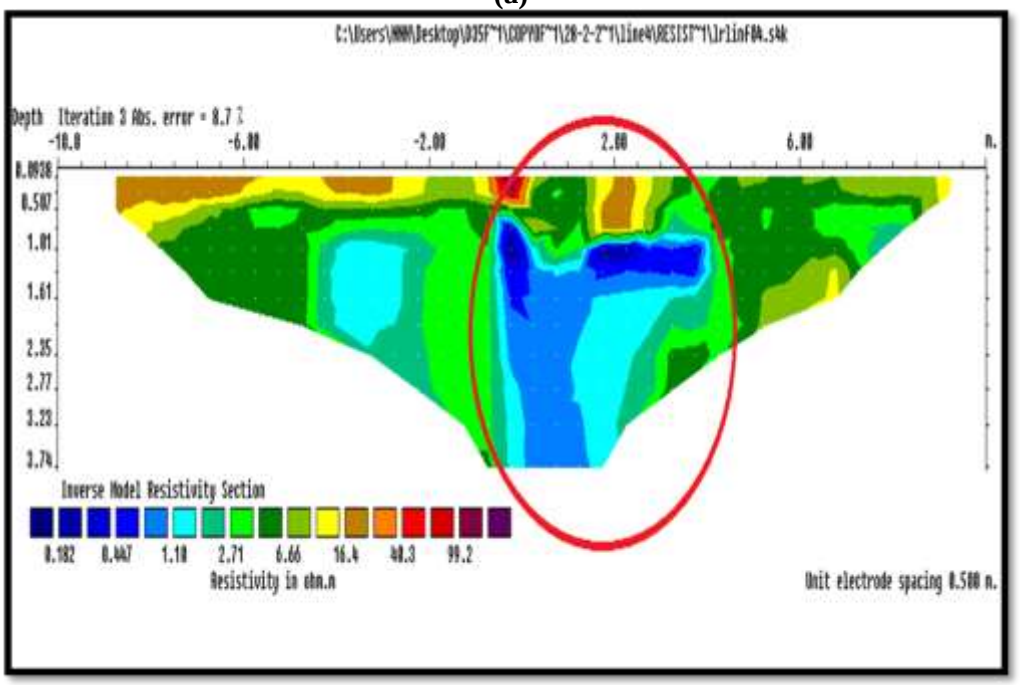

(b)

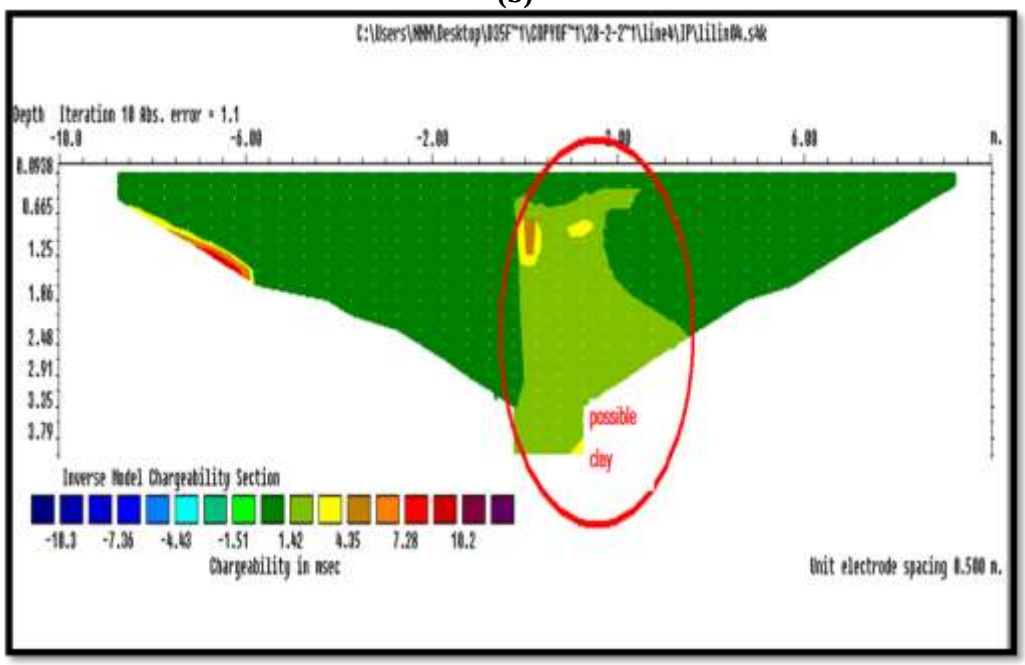

Figure (7) Inverted sections of LINE 4: (a) resistivity; (b) chargeability.

(a)

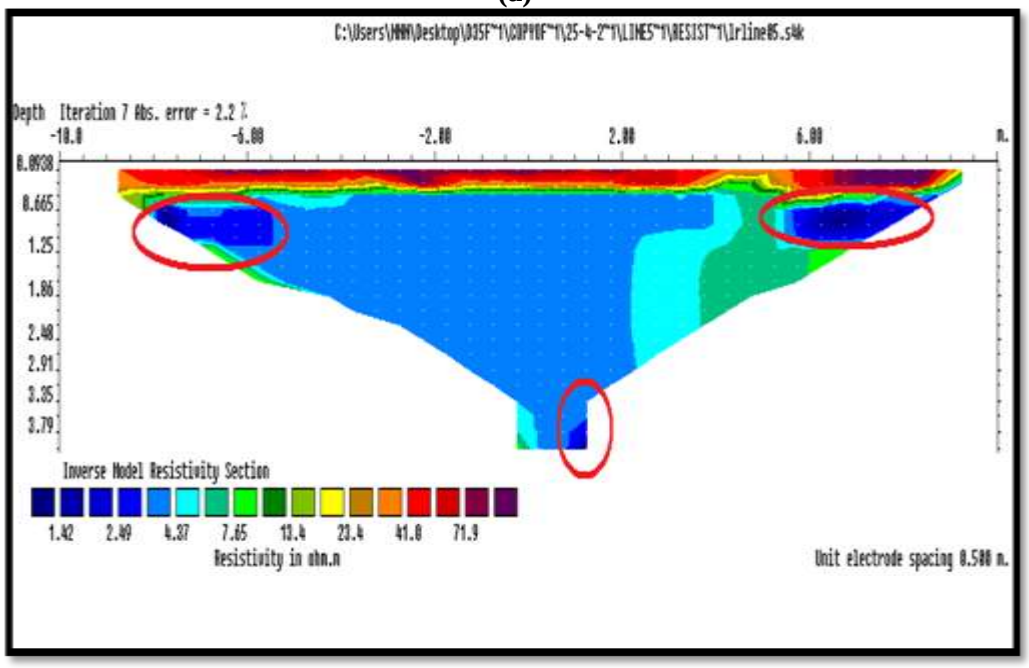

(b)

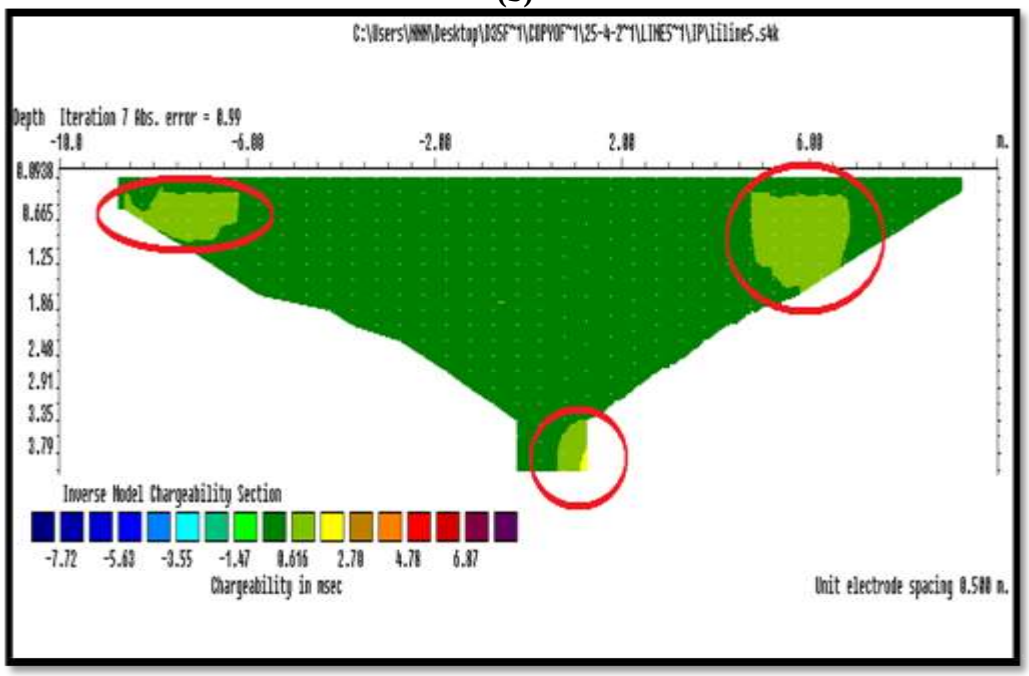

Figure (8) Inverted sections of LINE 5: (a) resistivity; (b) chargeability.

(a)

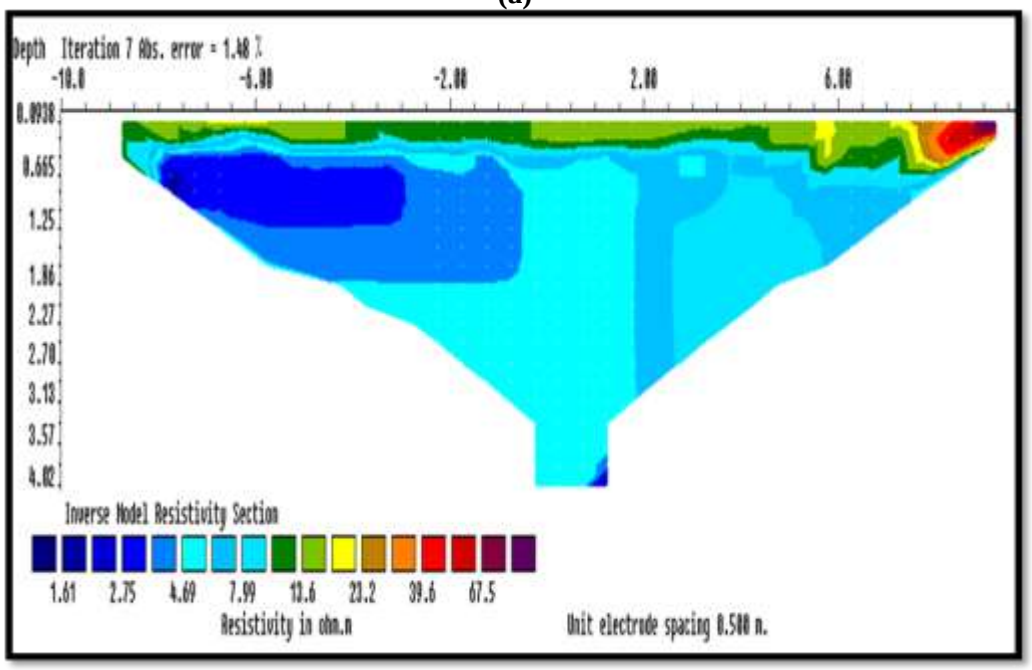

(b)

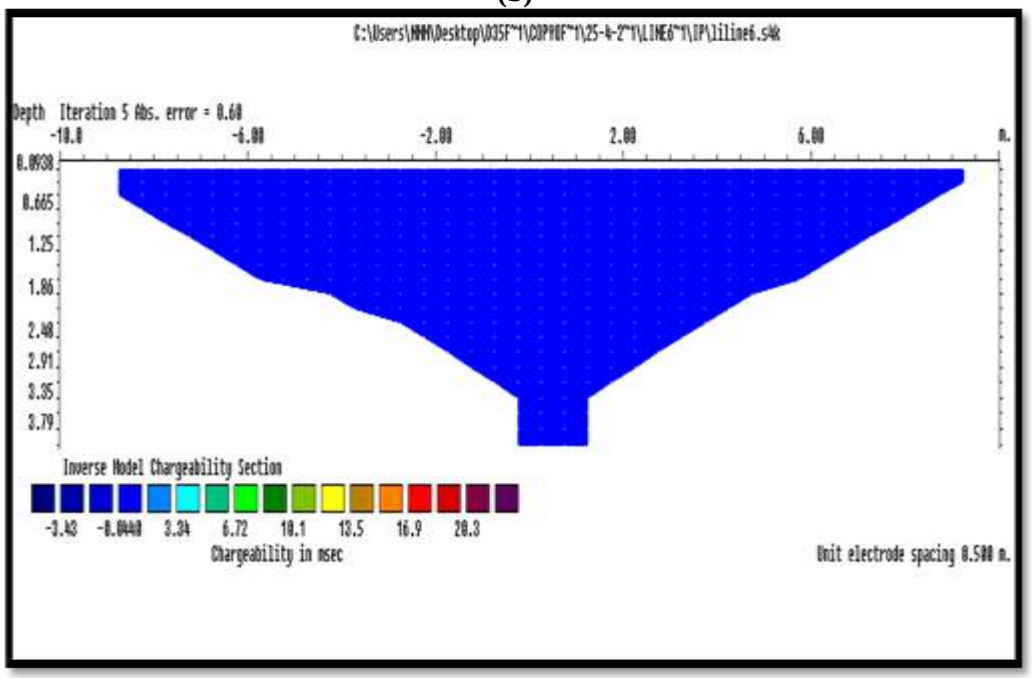

Figure (9) Inverted sections of LINE 6: (a) resistivity; (b) chargeability.

(a)

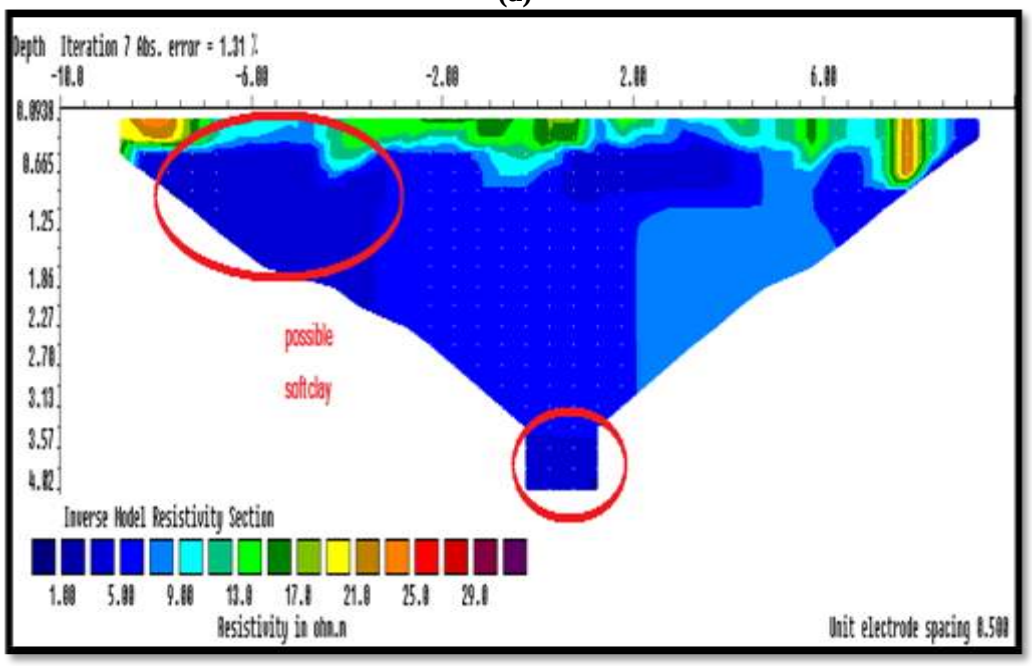

(b)

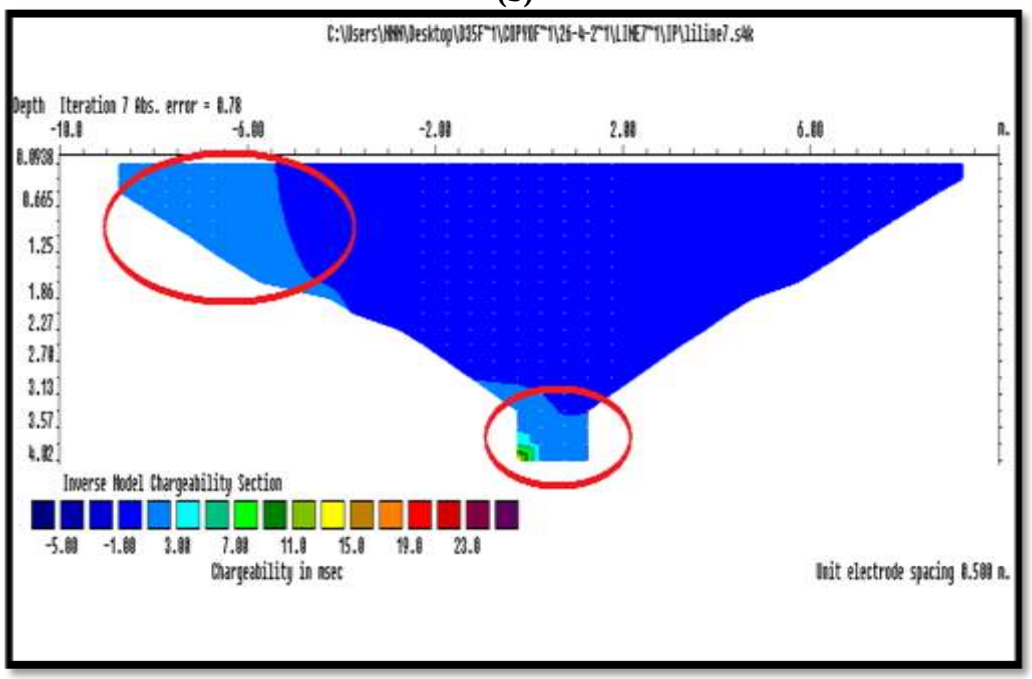

Figure (10) Inverted sections of LINE 7: (a) resistivity; (b) chargeability.